International Journal of Luminescence and Applications (ISSN: 2277-6362)
Vol. 5, No. 3, August 2015. Article ID: 120. pp.336-343.

Mechanoluminescence

B.P. Chandra[1*], V.K. Chandra[2] and **Piyush Jha[3]**

[1]*School of Studies in Physics and Astrophysics, Pt. Ravishankar Shukla University, Raipur, (C.G.), India*
[2]*Department of Electrical and Electronics Engg., Chhatrapati Shivaji Institute of Technology, Kolihapuri, Durg, (C.G), India*
[3]*Department of Applied Physics, Raipur Institute of Technology, Chhatauna, Mandir Hasuad, Raipur, (C.G.), India*

Abstract— *Mechanoluminescence (ML) is a type of luminescence induced by any mechanical action on solids. The cold light emissions induced by elastic deformation, plastic deformation and fracture of solids are called elastico ML (EML), plastico ML (PML), and fracto ML (FML), respectively. Whereas nearly 50% of all inorganic salts and organic molecular solids show ML during their fracture, only a few solids exhibit ML during their elastic and plastic deformation. The EML intensity of $SrAl_2O_4$:Eu, ZrO_2:Ti, and $Ca_2Al_2SiO_7$:Ce, and the FML intensity of europium tetrakis (dibenzoyl methide) triethynyl ammonium, ditriphenylphosphine oxide manganese bromide, freshly grown impure saccharin, etc. is so intense that it can be seen in day light with naked eye. The ML spectra consist of either the solid state luminescence spectra or the discharge spectra of surrounding gases or the combination of the both. The investigation of ML has become interesting because of its potential for sensing and imaging devices, light sources, multicolour displays, and many other mechano-optical devices. In the recent past, many new EML, PML and FML materials having intense ML have been investigated The present paper reports the salient features of elastico-, plastico- , and fracto- mechanoluminescences, and furthermore, discusses the devices, characteristics, and mechanisms of EML, PML and FML. The emerging applications of ML in the fields of energy, sensors and biology are also discussed, and perspectives for ML are described. In fact, the research in EML, PML and FML is rich with many possible experiments and applications.*

1. INTRODUCTION

It is not a fiction, but a scientific fact that strong light emission takes place during elastic deformation, plastic deformation and fracture of solids. In fact, the phenomenon of light emission induced by any mechanical action on solids is known as mechanoluminescence (ML). [1, 2], and the luminescence induced by elastic deformation, plastic deformation and fracture of solids are called elastico ML (EML), plastico ML (PML), and fracto ML (FML), respectively. The ML was probability first discovered when human lived in caves, since many common minerals produce very bright light emission. The first recorded discovery of ML was made by Francis Bacon, in 1605, who reported in his writings, *Advancement of Learning,* that "hard sugar being nimbly scraped with a knife would afford a sparkling light [1]." Till now, Chandra and his collaborators have reported the ML intensity, ML spectra, and ML-crystal-structure relationships of more than one thousand organic and inorganic crystals [1]. In recent years, ML has great potential for their applications in sensing, imaging, light sources, colour displays, and other mechano-optical devices. The present paper reports the salient features of elastico-, plastico-, and fracto-mechanoluminescence. It decribes the mechanoluminescent materials, devices for ML measurement, and characteristics, mechanisms, and mathematical understanding of EML, PML and FML. The emerging applications of ML in the fields of energy, sensors, and biology are discussed, and perspectives for ML are described.

** Corresponding Author Email: bpchandra4@yahoo.co.in*

2. MECHANOLUMINESCENT MATERIALS

2.1 Elastico-Mechanoluminescent Materials

The elasticomechanoluminescent materials known to date are [3]: ZnS:Mn, γ-irradiated alkali halide crystals, $SrAl_2O_4$:Eu, $SrAl_2O_4$:Eu,Dy, $SrAl_2O_4$:Ce, $SrAl_2O_4$:Ce,Ho, $SrMgAl_6O_{11}$:Eu, $SrCaMgSi_2O_7$:Eu, $SrBaMgSi_2O_7$:Eu, $Sr_2MgSi_2O_7$:Eu, $Ca_2MgSi_2O_7$:Eu,Dy, $CaYAl_3O_7$:Eu, $(Ba,Ca)TiO_3:Pr^{3+}$, $ZnGa_2O_4$:Mn, $MgGa_2O_4$:Mn, $BaAl_2Si_2O_8$:rare earth element, $Ca_2Al_2SiO_7$:Ce, ZrO_2:Ti,$CuZnO_5:Mn^{2+}$, $CaZr(PO_4)_2:Eu^{2+}$and ZnS:Mn, Te phosphors. The EML has also been observed in the nanoparticles of ZnS:Mn, $SrAl_2O_4$:Eu, ZnMnTe and $(ZnS)_{1-x}(MnTe)_x$. Certain materials such as $SrAl_2O_4$: Eu, $SrMgAl_6O_{11}$: Eu, $Ca_2Al_2SiO_7$: Ce, ZrO_2: Ti, etc., show such an intense EML that it can be seen in daylight with naked eye.

2.2 Plastico-Mechanoluminescent Materials

All the elastico-mechanoluminescent materials exhibit plastico ML. In addition, certain polymers, alkaline earth oxides, certain non-coloured alkali halide crystals, certain verity of rubbers, and certain metals also exhibit plastico ML [1,2].

2.3 Fracto--Mechanoluminescent Materials

Nearly 50% of all inorganic salts and organic molecular solids exhibit fracto ML. All elastico-

mechanoluminescent materials and all plastico-mechanoluminescent materials exhibit fracto ML. The fracto ML of europium tetrakis (dibenzoyl methide) triethynyl ammonium, ditriphenylphosphine oxide manganese bromide, freshly grown impure saccharin, etc. is so intense that it can be seen in day light with naked eye. The examples of intense fracto-mechanoluminescent materials are: $SrAl_2O_4$:Eu, Dy,. $SrMgAl_6O_{11}$:Eu, $Ca_2Al_2SiO_7$:Ce, ZrO_2:Ti, ditriphenyl phosphine oxide manganese bromide, europium tetrakis (dibenzoyl methide) triethyl ammonium, cholesteryl salicylate, N-isopropylcabazole, N-acetylanthranilic acid, cinchonine sulphate, cholesteryl salicylate, acenaphtnene, coumarin, phenanthrene, $Ce_2(SO_4)_3.8H_2O$, resorcinol, cholesterol, sorbitol hexa-acetate, uranyl nitrate $6H_2O$, m-aminophenol, sucrose, zinc acidbenzoate dehydrate, L- ascorbic acid,. tartaric acid, cinchonine acid, etc. [1,2].

3. DEVICES FOR ML MEASUREMENTS

Three kinds of devices are needed for the ML measurements; namely, devices for deforming the samples, devices for monitoring ML, and devices for spectral measurements. Different deformation techniques used for systematic measurement of the ML induced by deformation and fracture of solids are: compression technique, stretching technique, bending technique, pressure–step technique or loading technique, pressure–pulse technique, piston impact or impulsive technique, cleavage technique, etc. [1]. The ML intensity is measured using a photomultiplier tube or a semiconductor diode or a CCD camera. Image intensifier and dual detector spectrometer are used for recording the ML spectra. In recent years, non–intensified optical multichannel analyzers are being used, where mechanoluminescence is diffracted by grating and detected without signal amplification by the linear diode array. Sometimes interference filters are also used for recording the ML spectra. Using the ML devices the deformation, temporal, spectral, pressure, strain-rate, and other characteristics of the ML can be determined.

4. ELASTICO-MECHANOLUMINESCENCE OF PERSISTENT LUMINESCENT MATERIALS AND II-VI SEMICONDUCTORS

4.1 Characteristics of Elastico ML

Here, we describe the EML characteristics of persistent luminescent materials and ZnS:Mn films, which emit strong EML. The $SrAl_2O_4$:Eu,Dy and other persistent luminescent phosphors are prepared by solid state reaction technique in reduction atmosphere (Ar + 5% H_2). Then, they are ground and composites of desired shape are made by mixing 1.0 g of sintered powders and 3.5 g of epoxy resin of epichlorihydrine using a silicon mold. The thin film of ZnS:Mn nanoparticles having Mn^{2+} concentration of 1.5 percent and a mean size of 20 nm can be fabricated on various substrates by physical vapour deposition of ion plating or a sputtering method.

4.1.1 Persistent Luminescent Materials

i) *Deformation characteristics*— Fig. 1(a) shows the elastico ML behavior of UV-irradiated $BaSi_2O_2N_2$:Eu phosphor produced during application of a force of 20 kN (64 MPa) [4]. It is seen that, initially the EML intensity increases with the applied pressure, attains a peak value, and then it decreases with time. The EML of weak intensity also appears during the release of applied pressure.

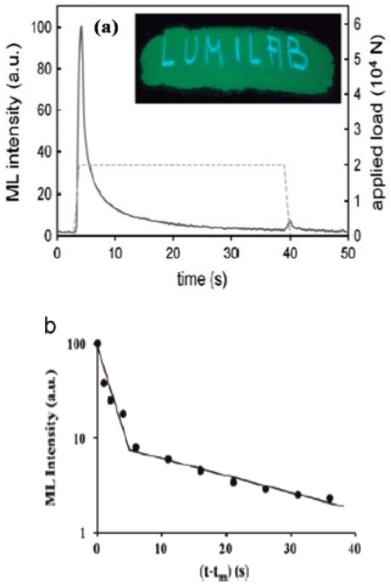

Fig. 1: (a) Typical EML behavior of stress-stimulated $BaSi_2O_2N_2$:Eu during application of a force of 20 kN (64 MPa). The solid line shows the EML intensity) and the dashed line shows the force profile. Inset shows the photograph taken after writing the name 'LUMILAB' on a layer of $BaSi_2O_2N_2$:Eu powder (after Botterman et al., Ref. [4]), (b) semilog plot of EML intensity I versus $(t-t_m)$.

ii) *Decay characteristics*— When the applied pressure is kept constant or released, then, as shown in Fig.1(b), initially the EML intensity decreases at a fast rate and then at a slow rate..

iii) *Pressure characteristics*— When pressure is applied at a fixed pressing rate, the EML appears after a threshold pressure and then the EML intensity increases linearly with the applied pressure.

iv) *Total EML intensity characteristics*— The total EML intensity increases linearly with the square of the applied pressure.

v) *Pressing rate characteristics*— The EML intensity increases linearly with the pressing rate of the crystals.

vi) *Trap concentration characteristics*— Both I_m and I_T increase with the concentration of filled electron traps in the crystals and consequently more electrons are detrapped for recombination.

vii) *Recovery characteristics*— In persistent luminescent materials the EML intensity decreases with the successive number of pressings because the concentration of filled electron traps decreases with the successive number of pressings. However, when the previously pressed samples exhibiting diminished EML intensity is exposed to UV-radiation, the recovery of initial EML intensity takes place because of the increase in the concentrations of filled electron traps. It is to be noted that, in the case of ZnS:Mn phosphors, the EML intensity does not change with the number of pressings.

viii) *Impulsive characteristics*— When a load of a fixed mass is dropped on to a sample from a fixed height, then initially the ML intensity increases linearly with time, attains a peak value and later on it decreases with time.

ix) *Activator concentration characteristics*— The EML is optimum for a particular concentration of activators.

x) *Volume characteristics*— The EML intensity increases with increasing volume of the sample.

xi) *Temperature characteristics*— The EML intensity should be optimum for a particular temperature of the crystals, but the effect of temperature on the EML of crystals has not been studied in detail till now.

xii) *Spectral characteristics*— As shown in Fig. 2, the EML spectra of $SrAl_2O_4$:Eu phosphor are similar to the photoluminescence spectra.

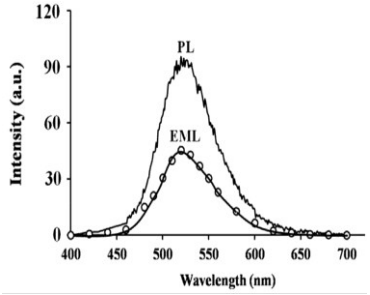

Fig. 2: EML, and photoluminescence spectra of $SrAl_2O_4$:Eu phosphor (for photoluminescence λexc=365nm).

xiii) *EML-TL correlation characteristics*— The EML intensity of $SrAl_2O_4$:Ho, Ce phosphor is higher as compared to that of $SrAl_2O_4$:Ce phosphor, and the thermoluminescence (TL) intensity of $SrAl_2O_4$:Ho,Ce phosphor is also higher as compared to that of $SrAl_2O_4$:Ce phosphor [5]. As higher TL intensity is related to the higher number of filled electron traps, the correlation between EML intensity and TL intensity indicates that for the crystals of similar structure and comparable piezoelectric constants the higher number of filled electron traps gives higher EML and TL intensities.

4.1.2 ZnS:Mn

i) Deformation characteristics— As shown in Fig. 8(a) when a load is applied on to the ZnS:Mn nanoparticles film coated on to a quartz substrate, then initially the EML intensity increases with time, attains a peak value and later on it decreases with time when the load tends to attain a fixed value [6]. It is seen that, when the pressure is released, then the EML emission also takes place. When the load is applied for the second time, then also the EML appears during the application and release of applied pressure, which shows the reproducibility of EML.

ii) *Decay characteristics*— Fig. 3(b) shows the semilog plot of the EML intensity I versus $(t-t_m)$ [6]. From the slopes of this semilog plot for lower and higher values of times, the values of fast (τ_1) and slow (τ_2) decay times are determined and they are found to be 1.69 and 5.88 s, respectively.

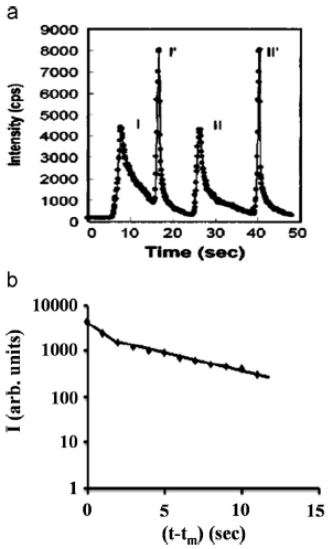

Fig. 3: (a) EML response of ZnS:Mn nanoparticles coated on quartz plate for the compression stress of 500 N, which was applied by material test machine with a cross-head speed of 0.10 mm/min. (after Xu et al. Ref.[6]), (b)plot of log I versus $(t-t_m)$ for ZnS:Mn nanoparticles for the ML induced by application of pressure of 500N.

iii) *Impulsive characteristics of EML*— When a load of 100 g is dropped on to ZnS:Mn nanoparticles film from a height of 10 cm, then initially the EML intensity increases linearly with time, attains a peak value and later on it decreases with time. In this case, also the semilog plot between the EML intensity I and $(t-t_m)$, is a straight line with a negative slope**.** Both I_m and I_T increase with increasing value of the height through which the ball is dropped on to the phosphor.

iv) *Pressing rate characteristics*— The EML intensity increases linearly with the pressing rate of the crystals.

v) *Strain rate characteristics of EML*— The EML intensity increases linearly with the strain rate of the crystals.

vi) *Spectral characteristics of EML*— Fig. 4 shows the ML, PL and EL spectra of II – VI semiconductors [7]. It is evident that the ML spectra are similar to the PL and EL spectra. This fact shows that although the excitation mechanism is different in ML, PL, and EL, the emission of photons occurs from the similar transitions.

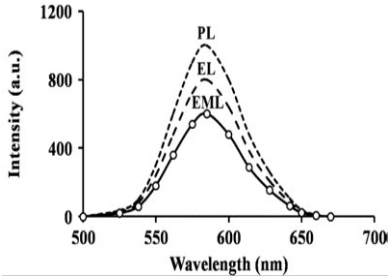

Fig. 4: EML, electroluminescence and photoluminescence spectra of ZnS:Mn phosphor (for photoluminescence λexc = 365 nm) [7].

4. MECHANISMS OF ELASTICO-MECHANOLUMINESCENCE

The EML of persistent luminescent materials and II-VI semiconductors can be understood on the basis of the trap-depth reduction model of elastico-mechanoluminescent materials.

As shown in Fig. 5 the EML of persistent luminescent materials where the dopant is rare earth ions such as Eu^{2+} can be understood with respect to the following steps [7]:

i) When a pressure is applied, one surface of the local piezoelectric region produced due to the impurities in the persistent luminescent material becomes positively charged and the other surface becomes negatively charged.

ii) The reduction in the trap-depth caused by the piezoelectric field causes detrapping of electrons whereby the detrapped electrons move to the conduction band.

iii) Some of the detrapped electrons moving in the conduction band recombine with the Eu^{3+} ions produced previously by UV-irradiation of persistent luminescent materials such as $SrAl_2O_4$:Eu and subsequently generate excited Eu^{2+} ions.

iv) The de-excitation of excited Eu^{2+} ions gives rise to the light emission characteristic of the luminescence centres.

Using Fig. 5 the EML of ZnS:Mn crystals can be understood with respect in the following way [7]:

i) As a result of the applied pressure one surface of a local piezoelectric region produced due to the impurities in ZnS:Mn crystal gets positively charged and the other surface gets negatively charged.

ii) Due to the reduction in trap-depth caused by the local piezoelectric field detrapping of electrons takes place, in which the detrapped electrons move to the conduction band.

iii) Some of the detrapped electrons moving in the conduction band recombine with the holes, in which the energy released during the electron-hole recombination excites Mn^{2+} ions.

iv) The de-excitation of excited Mn^{2+} ions gives rise to the light emission characteristic of the Mn^{2+} ions.

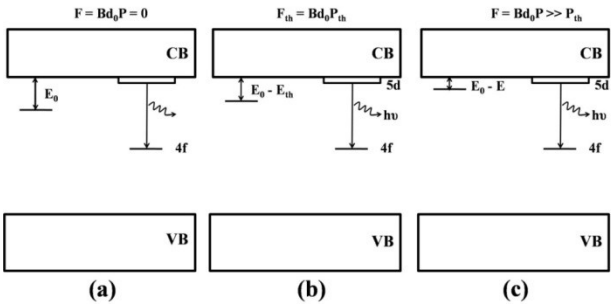

Fig. 5: Schematic diagrams for the reduction in trap-depth with the piezoelectric field F: (a) F = 0, (b) F = F_{th}, and (c) F >> F_{th}. Here, F_{th} is the threshold piezoelectric field for the EML emission, P_{th} the threshold pressure for the EML emission, d_0 the piezoelectric constant of the local region, P the applied pressure, and B the correlating factor between the piezpelectric field F and surface charge density d_0P [7].

5. PLASTICO-MECHANOLUMINESCENCE OF II-VI SEMICONDUCTORS

The PML of II-VI semiconductors and coloured alkali halide crystals have been studied in detail. Here, we describe the PML of II-VI semiconductors in detail. The PML of coloured alkali halide crystals have been reported by us in our other paper [8].

5.1 Characteristics of Plastico ML

i) *Deformation characteristics*— Fig. 6 (a, b, c) shows the ML-strain and stress-strain curves of ZnS:Mn crystals at a fixed strain rate. It is seen that the ML appears in the elastic region as well as in the plastic region [9]. Initially, the ML intensity increases with time and then it tends to attain a saturation value for larger value of the deformation. It is evident from Fig. 6(c) that the ML pulses appear concurrently with the steps occurring in the stress-strain curve of the crystal. As the step in the stress -strain curve is related with the movement of dislocations, it seems that the moving dislocations are responsible for the ML emission in ZnS:Mn crystals.

Fig. 7 shows the dependence of the ML intensity on the deformation of ZnS: Cu, Al single crystal [10], where deformation is performed at a fixed strain rate. It is seen that the ML does not appear in the elastic region; however, it appears in the plastic region

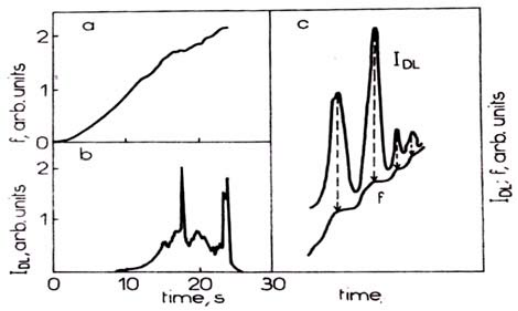

Fig. 6: Mechanoluminescence IML of a crystal of ZnS :Mn deformed in bending at a rate of 8.4 x 10-7 ms-1 under a load f (c) is a magnified portion of the two curves shown in (a) ans (b) (after Alzetta et al. [9]).

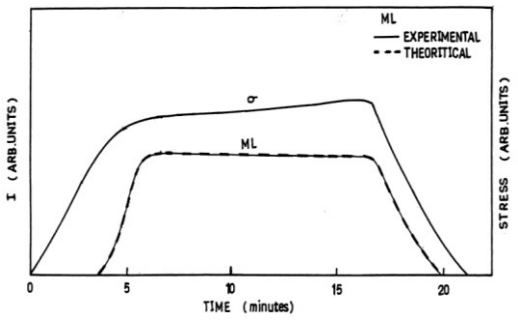

Fig. 7: ML intensity versus deformation time and stress versus deformation time curves of ZnS:Cu,Al crystal deformed at a strain rate of 10 μm/min (after Bredikhin and Shmuralk, ref. [10]).

ii) *Decay characteristics*— The semilog plot between the PML intensity and $(t-t_c)$ is a straight line with a negative slope, in which the decay gives the pinning time of dislocations. rse of the slope of this plot the value of the pinning time of dislocations is determined and it is found to be 90.91 sec.

iii) *Thermal characteristics*— The decrease in the ML intensity with temperature is faster as compared to that of the photoluminescence (PL) intensity. As the ML intensity depends on η and charge density of the dislocations or the radius of the interaction between charged dislocation and filled electron traps; however, the PL intensity depends only on η, and both η and the charge density of the dislocations decrease with temperature, a faster decrease of ML intensity as compared to that of the PL intensity occurs with increasing temperature of the crystals.

iv) *Spectral characteristics*— The ML spectra are similar to their EML spectra as shown in Fig. 4. In this case, also the PML spectra are similar to their PL and EL spectra.

v) *Strain rate characteristics*— The ML intensity of ZnS: Mn crystals increases linearly with the strain rate.

vi) *Concentration characteristics of*— Initially the ML intensity increases with increasing concentration of Mn as the number of luminescence centres increases; however, for higher concentration of Mn the ML intensity decreases because of the concentration quenching. Thus, the ML intensity is optimum for a particular concentration of Mn in ZnS.

5.2 Mechanism of Plastico ML of II-VI Semiconductors

The ML of II – VI semiconductors during plastic deformation occurs in the following steps [1, 10] :

i) The plastic deformation causes movement of dislocations.

ii) The electric field of the charged dislocations, which is of the order of 10^8 V/cm, causes bending of the valance band and conduction band as well as dislocation bands.

iii) Subsequently, the electrons from the electron trap tunnel to the conduction band

iv) The energy released during the recombination of electrons with the holes gives rise to the light emission characteristic of the activator centres. In the case of Mn doped II – VI semiconductors, the energy released during the electron-hole recombination excites Mn^{2+} ion and the subsequent de-excitation gives rise to the light emission characteristic of Mn^{2+} ions.

6. FRACTO-MECHANOLUMINESCENCE OF ORGANIC AND INORGANIC CRYSTALS

6.1 Characteristics of Fracto ML

i) *Deformation characteristics*— Fig. 8 shows the ML versus compression curve and force versus compression curve of a tartaric acid crystal [11]. It is seen that the ML appears concurrently with the steps occurring in the force versus compression curve of the crystal. As the steps in the force versus compression curve correspond to the movement of a crack in the crystal, it seems that the creation of new surfaces is responsible for the ML emission.

ii) *Impact characteristics*— Fig 8 (a) shows that, when a fluorescent N-acetylanthranilic acid (NAAA) crystal is fractured by the impact of a moving cylinder of mass 400 gm, then initially the ML intensity increases linearly with time, attains a peak value I_m at a particular time t_m and later on it

decreases with time. The time dependence of the ML intensity of sugar crystals is also similar to that of NAAA crystals.

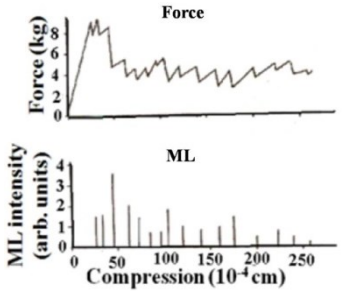

Fig. 8: ML-compression and force-compression curves of 6×5×4 mm^3 tartaric acid single crystal (rate of compression =1.69x10-3 mm s-1) (after Chandra and Zink, ref. [11]).

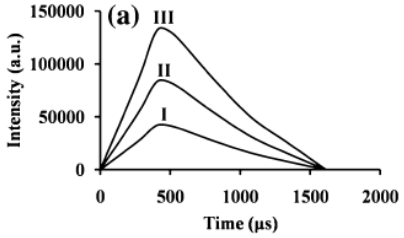

Fig. 9: (a) Time dependence of the ML intensity of 2 x 2 x 2 mm^3 fluorescent N-acetylanthranilic acid crystals (Curves I, II and III correspond to the impact velocity 99, 198 and 313 cm/s respectively),

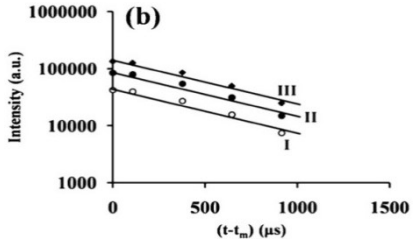

Fig. 9: (b) Semilog plot of ML intensity versus time for 2 x 2 x 2 mm^3 fluorescent N-acetylanthranilic acid crystals (Curves I, II and III correspond to the impact velocity 99, 198 and 313 cm/s, respectively.

iii) *Decay characteristics*— Fig. 9 (b) shows the semilog plot of I versus (t-t_m) for NAAA crystal is straight line with negative slope and the value of slope does not change significantly with increasing value of the impact velocity of the cylinder used to deform the crystals. The value of ML decay time $1/\xi$ is determined from the slope of this plot for different values of the impact velocity v_0, and it is found to be 555 μs and 526 μs, respectively for NAAA and sugar crystals, respectively.

iv) *Peak ML intensity characteristics*— The peak ML intensity I_m crystals initially increases linearly with increasing impact velocity of the piston used to deform the crystals; however, it tends to attain a saturation value for high impact velocities.

v) *Total ML intensity characteristics*— The total ML intensity I_T of crystals initially increases with increasing impact velocity of the piston used to deform the crystals; however, however, it tends to attain a saturation value for high impact velocities.

vi) *Peak time characteristics*— The peak time tm does not change significantly with changing the height of the piston through whichthe piston is dropped on to the sample.

vii) *Impact characteristics of ML excited by a moving ball*— Both I_m and I_T initially increase quadratically with the impact velocity v_0; however, it tends to attain a saturation value for high impact velocities. The value of t_m is not affected significantly with v_0.

viii) *Surface area characteristics*— The total ML intensity increases linearly with the atea of newly created surfaces of the crystals by fracture.

ix) *Spectral characteristics*— Depending on the prevailing conditions the ML spectra consist of the solid state luminescence spectra or gas discharge spectra or the combination of the both.

6.2 Mechanisms of Fracto ML of Crystals

The fracto ML can be understood on the basis of the Langevin model for the creation of charged surfaces during the movement of a crack in a piezoelectric crystal, shown in Fig. 10 [12]. When a crack moves in a piezoelectric crystal, one of the newly created surfaces gets positively charged and the other surface gets negatively charged in which a strong electric field is generated between the two walls of a crack. The piezoelectric constant is generally of the order of 10^{-12} - 10^{-11} Coulomb per Newton (CN^{-1}) and the stress needed to separate the surfaces of crystals is of the order of Y/100 (where Y is the Young's modulus of elasticity of the crystal), which comes out to be order of 10^8 Nm^{-2}. Thus, the charge density ρ of the newly created surfaces is of the order of 10^{-4}-10^{-3} Coulomb m^{-2}. The electric field F between the oppositely charged surfaces will be, $F = \rho / \varepsilon_o$, where ε_o is the permittivity of free space, equal to 8.85×10^{-12} $C^2N^{-1}m^{-2}$. Thus, an electric field of the order of 10^7-10^8 Vm^{-1} may be generated between the newly created oppositely charged surfaces. This field may cause the dielectric breakdown of the surrounding gases and in turn may give rise to the gaseous discharge ML. The field may also cause the dielectric breakdown of the crystals, and the recombination of free charge carriers may give rise to recombination luminescence. Furthermore, the accelerated electrons moving from negatively charged surfaces towards the positively charged surface may excite cathodoluminescence (CL).

In addition to the piezoelectric crystals, a large number of non-piezoelectric crystals also exhibit ML. Thus, it seems that the charging of newly created surfaces also takes place due to some other processes such as the movement

of charged dislocations, baro-diffusion of defects in crystals, local piezoelectric field caused by impurities and defects, creation of non-centrosymmetric structure by the stress required for fracture, local piezoelectric field caused by the large strain at fracture, fracturing of centrosymmetric ionic crystals in a direction which actually generates charged surfaces, the presence other phases in solvated materials, presence of non-centrosymmetric phase due to disorder in materials, charging of the sites (like oxygen, halogen, etc) of different electro-negativity in neutral polar molecules, etc.

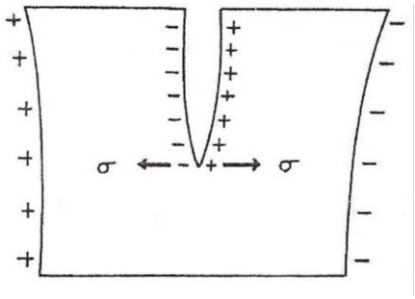

Fig. 10: Piezoelectrification model of fracto ML.

If there is total transfer of energy from the excited gas molecules to the luminescence centres or the light produced due to gas discharge is absorbed completely by the crystals, then only the solid state FML will be produced. Moreover, if the electric field will not be sufficient to cause the gas discharge, then also the gas discharge FML will not be observed. Furthermore, if the surface charges relax before the penetration of gases between the walls of the cracks, then also the gas discharge ML will not be observed. On the other hand, if there is partial transfer of energy from the excited gas molecules to the luminescence centres or partial absorption of the light produced due to the gas discharge by the crystals, then the combination of both the solid state FML and gas discharge FML will be observed. Furthermore, if the crystals do not possess luminescence centres, then there will be no transfer of energy from the excited gas molecules to the luminescence centres or absorption of gas discharge by the luminescence centres, and in this case only the gas discharge FML will be observed. Thus, depending on the prevailing conditions either gas discharge or FML resembling other types of luminescence or combination of these two may be obtained.

7. APPLICATIONS OF ML

The important applications of ML are as given below:

7.1 EML

(i) Stress sensor, (ii) real- time visualization of the stress distribution in solids, (iii)visualization of internal defect in a pipe, (iv) analysis of the artificial legs, (v) real-time visualization of the quasidynamic crack-propagation in solids, (vi) determination of the crack-growth resistance and other parameters of crack- propagation, (vii) novel ML-driven solar cell system, (viii) real-time visualization of the stress field near the tip of a crack, (ix) pressure mapping of handwriting using EML pressure sensor matrix (PSM) device [13], (x) ML light sources and displays [14-16], (xi) determination of laser and ultrasonic powers, (xii) secret message writing, (xiii) EML-based safety-management monitoring system, and (xiv) radiation dosimetry.

7.2 PML

(xv) Non- destructive testing of materials [1], (xvi) useful in the photography as well as in the writing of secret messages, (xvii) gives information about the stress and strain corresponding to the yield point of crystals, (xviii) gives information about the slip planes of the crystals, (xix) visualisation of Portevin–Le Chatelier effect using mechanoluminescent sensing film, and (xx) sensing the formation and propagation of Lüders bands.

7.3 FML

(xxi)Mechanoluminescence damage sensors, (xxii) fracture sensors, (xxiii) impact sensors, (xxiv) fuse-system for army-warhead, (xxv) evaluation of the design of milling machine, (xxvi) online monitoring of grinding process, (xxvii) fragmentation studies of solids, (xxviii) potential for earth quake indicator, (xxix) determination of several parameters of solids, and (xxx) triboluminescence X- ray unit has been designed for X – ray imaging (xxxi) Micrometeoroid and ultra high speed (hypervelocity) debris impacts pose a significant threat to a spacecraft. Mechanoluminescence has the potential to be used to detect impacts and other phenomena for space applications, (xxxii) ML-based structure health monitoring system, (xxxiii) electronic structure of metal surfaces, and (xxxiv) determination of shock-wave velocity, shock pressure, transit time of shock-wave, decay time of surface charges, etc.

8. CONCLUSIONS

The investigation of ML has become interesting because of its potential for sensing and imaging devices, light sources, multicolour displays, and many other mechano-optical devices. The investigation of ML-based damage sensor and ML-based safety management monitoring system are considered to be a great achievement in the field of ML. Thus, the research in EML, PML and FML is rich with many possible experiments and applications.

REFERENCES

[1] B.P. Chandra, Mechanoluminescence, in Luminescence of Solids, D. R. Vij (Ed.), Plenum Press, New York, 1998, pp 361-389.

[2] B.P. Chandra, Mechanoluminescent Smart Materials and their Applications, in Electronic and Catalytic Properties of Advanced Materials, edited by A. Stashans, S. Gonzalez and H. P. Pinto, Transworld Research Network, Trivandrum, Kerala, India, 2011, pp.1-37.

[3] B.P. Chandra, V.K. Chandra, Piyush Jha, Physica B 463(2015) 62.

[4] J. Botterman, K. V. Eeckhout, I. De Baere, D. Poelman and P. F. Smet, Acta Materialia 60 (2012) 5494.

[5]] H. Zhang, H. Yamada, N. Terasaki and C.N. Xu, Appl. Phys. Lett. 91 (2007) 081905-1.

[6] C.N. Xu, T. Watanabe, M. Akiyama and X.G. Zheng, Appl. Phys. Lett. 74(1999)1236.

[7] B.P.Chandra, V.K.Chandra and Piyush Jha, Physica B 461(2015)38.

[8] B. P. Chandra, R. K. Goutam, V. K. Chandra, R. P. Patel, A. K. Luka and R. N. Baghel, Optoelectronics and Advanced Materials Rapid 3 (2009) 1181.

[9] G. Alzetta, I. Chudasek and R. Scarmozinno, Phys Stat Sol (a) 1 (1970) 775.

[10] S. I. Bredikhin and S. Z. Shmurak, Sov Phys JETP 49 (1979) 20.

[11] B. P. Chandra V.K. Chandra and Piyush Jha, Sensors and Actuators A:Physical 230 (2015) 83.

[12] B.P. Chandra, V.K. Chandra and P. Jha, J. Lumin. 135 (2013) 139.

[13] X. Wang, H. Zhang, R. Yu, L. Dong, D. Peng, A. Zhang, Y. Zhang, H. Liu, C. Pan and Z. L. Wang, Adv. Mater. 2015, DOI: 10.1002/adma.201405826.

[14] S.M. Jeong, S.Song, S.K. Lee and B. Choi, Appl. Phys. Lett.102 (2013)051110.

[15] S.M. Jeong, S. Song, S.K. Lee and N.Y. Ha, Adv. Mater. 25 (2013) 6194.

[16] S.M. Jeong, S. Song, K. Joo, J. Kim, S.H. Hwang, J. Jeong and H. Kim, Energy Environ. Sci. 7 (2014) 3338.